

Near-Field Light Design with Colloidal Quantum Dots for Photonics and Plasmonics

Stephan J. P. Kress,[†] Patrizia Richner,[‡] Sriharsha V. Jayanti,[†] Patrick Galliker,[‡] David K. Kim,[†] Dimos Poulikakos,[‡] and David J. Norris*,[†]

[†]Optical Materials Engineering Laboratory and [‡]Laboratory of Thermodynamics in Emerging Technologies, ETH Zurich, 8092 Zurich, Switzerland

 Supporting Information

ABSTRACT: Colloidal quantum-dots are bright, tunable emitters that are ideal for studying near-field quantum-optical interactions. However, their colloidal nature has hindered their facile and precise placement at desired near-field positions, particularly on the structured substrates prevalent in plasmonics. Here, we use high-resolution electro-hydrodynamic printing (<100 nm feature size) to deposit countable numbers of quantum dots on both flat and structured substrates with a few nanometer precision. We also demonstrate that the autofocusing capability of the printing method enables placement of quantum dots preferentially at plasmonic hot spots. We exploit this control and design diffraction-limited photonic and plasmonic sources with arbitrary wavelength, shape, and intensity. We show that simple far-field illumination can excite these near-field sources and generate fundamental plasmonic wave-patterns (plane and spherical waves). The ability to tailor subdiffraction sources of plasmons with quantum dots provides a complementary technique to traditional scattering approaches, offering new capabilities for nanophotonics.



KEYWORDS: Semiconductor nanocrystals, colloidal quantum dots, nanophotonics, plasmonics, electro-hydrodynamic printing

Colloidal quantum dots, also known as semiconductor nanocrystals, exhibit optical properties tunable with their size.¹ Consequently, after several decades of development they now provide efficient photostable emitters at almost any wavelength. For example, by controlling the diameter of CdSe quantum dots between 2 and 5 nm, narrowband fluorescence can be obtained that is tunable over the entire visible range.² For emission spanning the ultraviolet (UV) or infrared, nanocrystals of other semiconductors can be used.^{3–6} Thus, quantum dots offer emitters with spectra that can be freely designed.⁷ However, while this ability has been exploited in applications such as solid-state lighting⁸ where thin films of nanocrystals are used, applications that also take advantage of the small size of individual nanocrystals (e.g., biolabeling^{9,10}) are much less common.

One area that could benefit from the small size of quantum dots is nanophotonics.^{11–14} This field investigates light-matter interactions at length scales below the diffraction limit of light for applications ranging from sensing^{15–18} to high-resolution optical microscopy.^{19–22} Typically, conventional lasers are utilized as the light source. Photons from the far field must then somehow be coupled to local electromagnetic modes of interest. In metallic nanophotonic devices, these modes usually involve surface plasmon polaritons (SPPs), electromagnetic resonances that exist at a metal–dielectric interface.^{23–25} However, because a momentum mismatch exists that prohibits far-field photons from coupling directly to SPPs on a flat metallic surface, the metal must be structured to allow

excitation of SPPs via scattering (i.e., diffraction). This explains in part the use of bumps, grooves, apertures, nanoparticles, and so forth in plasmonic devices. When illuminated by a laser, such structures can provide near-field sources of either SPPs or photons at the same energy as the incoming light.

If quantum dots are placed at specific locations in nanophotonic structures, they can provide an alternative approach to near-field light sources.²⁶ Instead of using scattering as the in-coupling mechanism, the broadband absorption of the quantum dots can be utilized. The nanocrystals can simply be illuminated by a light source from the far field, creating excited quantum dots that then emit SPPs or photons. Because the semiconductor nanocrystals can be excited with photon energies well above their effective band gap, these outgoing SPPs or photons would not need to have the same energy as the incoming light. Nanocrystals of different colors could also be excited simultaneously with the same UV light source. If properly placed in the structure, these excited nanocrystals would then be sitting in the local mode of the photonic or plasmonic resonance of interest, allowing their quantum-optical interactions to be studied or utilized.

However, despite these advantages, colloidal quantum dots have not been fully exploited as nanoscale light sources in nanophotonics. This is due in part to the practical difficulty of

Received: July 16, 2014

Revised: August 27, 2014

Published: September 2, 2014

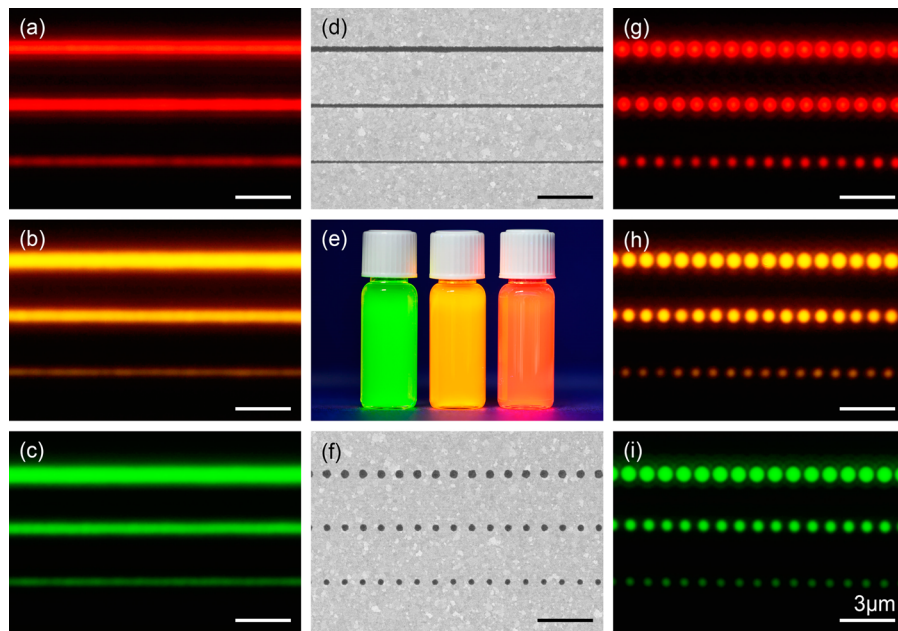


Figure 1. Optical images (fluorescence) and electron micrographs of CdSe/ZnS core/shell quantum dots placed on a flat template-stripped Au substrate from tetradecane dispersions via electro-hydrodynamic printing (EHD NanoDrip printing). (a–c) Fluorescent lines of 220, 150, and 100 nm widths in each obtained by varying voltage-pulse parameters and the number of overprints. (d) Scanning electron micrograph showing the subdiffraction size and high fidelity of the deposits. (e) Vials containing the three CdSe/ZnS quantum-dot inks. The quantum-dot-core diameters were 2.7, 3.4, and 5.1 nm for green (540 nm), orange (580 nm), and red (630 nm) fluorescence under UV excitation. Each had a shell thickness of approximately 1.7 monolayers. In addition to lines, spots (f–i) can similarly be printed.

placing colloidal particles with high specificity at desired locations. Any successful deposition technique must transfer nanometer-sized quantum dots, which are undergoing Brownian motion in liquid dispersions, onto a dry substrate, preferably with nanometer precision. To avoid the inherent difficulty of such positioning many studies have simply used random placement of the quantum dots.²⁶ Others have utilized stamping,^{27,28} self-assembly,²⁹ or multistep electron-beam-lithography techniques^{30,31} to gain some control. Unfortunately, all of these approaches are easily applicable only to planar substrates. This is a severe limitation for nanophotonics where structured devices are used not just to enable in-coupling via scattering (as discussed above) but also to allow the concentration of light into subdiffraction volumes.^{14,32–34} For example, localized plasmonic resonances exist at sharp tips, edges, and gaps on patterned metallic surfaces. Although nano-optical tweezers have been employed to electromagnetically guide single nitrogen-vacancy (NV) centers to such locations,^{35,36} these techniques cannot easily place quantum dots (which are an order of magnitude smaller than the NV centers) at such locations. Thus, a need exists for simple methods that can position quantum dots with subdiffraction resolution and nanometer precision, irrespective of how the photonic substrate is structured. This would then allow the arbitrary design of near-field quantum-dot light sources with the ability to control their color, shape, intensity, and location on both flat and structured substrates for plasmonic and photonic studies and applications.

Here, we demonstrate a simple solution to this problem. We utilize an electro-hydrodynamic printing technique^{37,38} to generate subdiffraction quantum-dot light sources. Because our technique works on both flat and structured substrates, all constraints of earlier deposition techniques are circumvented. Indeed, on structured metallic films, our technique can

automatically deposit the quantum dots at electromagnetically interesting positions due to an “electrostatic guiding” effect. Below, we demonstrate the flexibility of our approach by creating several simple quantum-dot plasmonic devices. We then analyze the ability of the quantum dots to generate arbitrary wave-patterns of surface plasmons.

For our experiments, we prepared two different types of quantum dots, CdSe/ZnS and CdSe/CdS core/shell nanocrystals. Three different sizes of CdSe cores were synthesized by adapting a known protocol³⁹ (see Supporting Information for details). After isolating the cores, they were then overcoated either with a ZnS shell⁴⁰ or with a CdS shell.⁴¹ The resulting core/shell nanocrystals were isolated through several cycles of precipitation and then redispersed in hexane for storage (see Figure S1 in the Supporting Information). Such core/shell quantum dots were utilized because they are efficient emitters with near-unity fluorescence quantum yields (~90%). To obtain an ink for printing, the quantum dots were subsequently transferred into tetradecane and their concentration was adjusted so that the optical density at the lowest-energy-exciton peak was 0.5 for a 1 mm path length. We note that reproducible high-resolution printing of the quantum dots required careful preparation of concentration-adjusted inks free of any excess of the surface ligands used to stabilize the colloidal particles.

To print these inks, we exploited a process known as electro-hydrodynamic (EHD) NanoDrip printing. Previously, it has been used to deposit primarily metal nanoparticles on flat substrates.^{37,38} Figure S2 in the Supporting Information shows a schematic of the printing setup. It utilizes a Cr/Au-overcoated glass pipet that is thermally drawn down to a tip with an opening of 500 to 1500 nm. After filling this pipet with a printing dispersion (ink), it is brought close to a substrate with a piezoelectric stage and used as a printing nozzle. By attaching

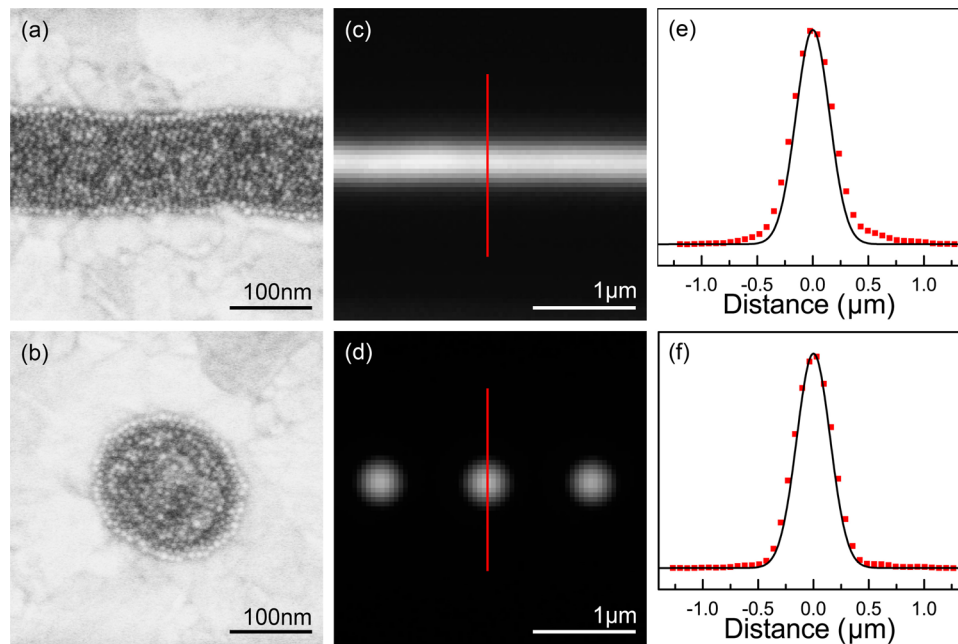


Figure 2. Electron and optical micrographs for quantitative analysis of highly fluorescent CdSe/CdS core/shell quantum dots printed on flat template-stripped Au surfaces. The quantum dots (made from 3.4 nm CdSe cores) are 8 nm in diameter (including the shell) and have a fluorescence peak at 629 nm. High-resolution scanning electron micrographs of printed (a) lines and (b) spots. A countable number of individual CdSe/CdS core/shell quantum dots are arranged within a densely packed layer on a smooth Au substrate with widths of 120 nm (lines) and 180 nm (spots). Fluorescence images of the printed (c) lines and (d) spots recorded with a cooled sCMOS camera (Hamamatsu Flash 4.0, pixel size 6.5 μm) and a high-numerical-aperture (NA) microscope objective (Nikon 100 \times , 0.9 NA, air immersion). Cross sections of the images (indicated with the red vertical lines) are plotted with red points in (e,f). The Gaussian line widths expected for an ideal point source in our apparatus are shown with black solid lines. The measured line widths for the printed structures are within 10% of ideal point sources, indicating the subdiffraction nature of the deposits.

a voltage source to the pipet and applying a pulse of around 250 V, attoliter-sized droplets of the ink can be ejected from the nozzle at rates of 0.1 to 1 kHz. By controlling the droplet ejection and the position of the pipet, patterns can be printed on the substrate. Au-nanoparticle deposits (both in and out of plane) with feature sizes down to 50 nm have been demonstrated.^{37,38}

Figure 1 shows fluorescence images and electron micrographs of printed lines (Figures 1a–d) and spots (Figures 1f–i) using inks prepared from our three different colors of CdSe/ZnS core/shell quantum dots (Figure 1e). In these experiments, the nozzle was brought within 5 μm of a flat template-stripped^{42,43} gold surface (root-mean-squared roughness <1 nm). For the lines, the nozzle was translated at speeds of 10 μm per second. For the spots, the nozzle remained steady for 25–500 ms while attoliter-sized droplets (~100 nm in diameter) were ejected. According to the concentration of the quantum dots in the ink, each droplet should contain only a few quantum dots. However, evaporation at the nozzle preconcentrates the quantum dots prior to droplet ejection. The size and fluorescence intensity of the printed lines and spots can be controlled by varying the printing parameters, such as the magnitude of the voltage pulse, the translation speed of the nozzle, the number of overprints, and so forth. An important feature of the method is that if these parameters are fixed, the printing process is extremely reproducible, both for a given ink (see Figure S3 in the Supporting Information) as well as different inks (i.e., different-sized quantum dots). For example, quantum-dot lines with widths of 220, 150, and 100 nm are demonstrated for all three inks in Figure 1. The data confirm that irrespective of the quantum-dot color (and thus size), this

technique can consistently print the same lines and spots down to subdiffraction resolutions exceeding 200 000 dots-per-inch (dpi). This offers great flexibility for the generation of light patterns on plasmonic and photonic surfaces.

A more detailed analysis of the quantum-dot deposits on flat Au substrates is presented in Figure 2. High-resolution scanning-electron micrographs reveal individual quantum dots within the 120 nm wide lines (Figure 2a) and 180 nm spots (Figure 2b). By counting the nanocrystals, we find that this width corresponds to ~15–20 quantum dots, which are assembled in a densely packed layer. Thus, EHD NanoDrip printing not only allows high-resolution deposits but produces films with qualities usually associated with spin- and dip-coating. This is advantageous for nanophotonics where the concentration of the emitters can be important for exploring light-matter interactions. Furthermore, fluorescence images confirm that these assemblies remain highly emissive (Figure 2c,d). A high-numerical-aperture (NA) microscope objective (Nikon 100 \times , 0.9 NA, air immersion) was used to image epifluorescence on a cooled sCMOS camera (Hamamatsu Flash 4.0, pixel size 6.5 μm). Cross sections from these images are shown in Figure 2e,f. The experimental data (red points) exhibit line widths that are within 10% of an ideal point dipole (solid line). Because any image may be decomposed into such ideal point sources, the ability to print nearly ideal point sources means that any light-pattern may be generated using this technique. Thus, these results again indicate that the printed deposits provide extremely flexible subdiffraction light sources.

Moreover, the printing parameters and the quantum-dot concentration can be adjusted to decrease the feature size

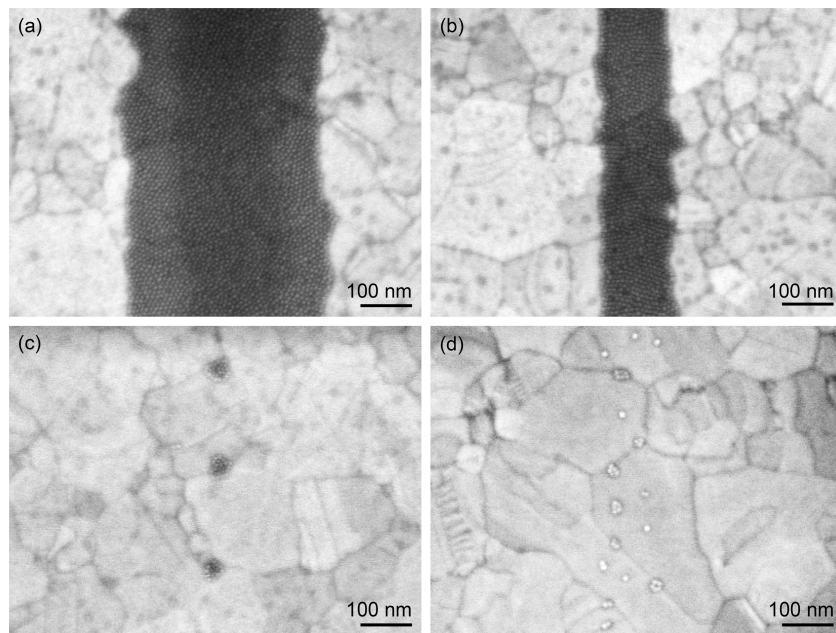


Figure 3. High-resolution scanning electron micrographs demonstrating deposition of sparse quantum dots on flat template-stripped Au surfaces. The quantum dots are as in Figure 2. Using concentrated ink (see Supporting Information for details) and 230 V for droplet ejection, continuous lines of quantum dots of different widths were obtained by translating the piezo-stage at (a) 50 and (b) 200 μm per second. The latter was the maximum usable speed for our stage. To decrease the number of quantum dots further, we maintained this speed and diluted the concentrated ink (1:10). In (c), 150 V resulted in 30 nm spots, each containing 10–20 quantum dots. In (d), 230 V led to deposits containing only a few or individual quantum dots.

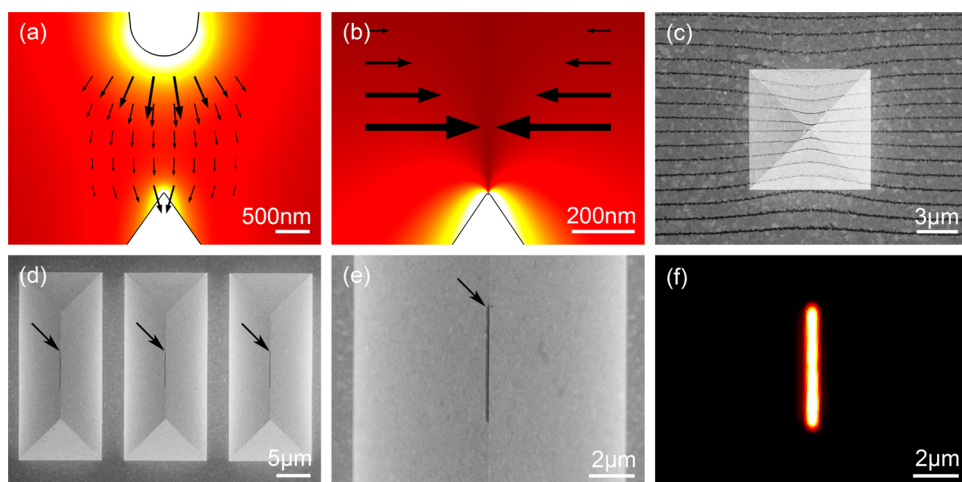


Figure 4. Simulations and electron micrographs illustrating autofocusing during printing of CdSe/CdS core/shell quantum dots onto structured plasmonic substrates. (a) Axi-symmetric electrostatic simulations of the total electric field (magnitude and field lines shown) between the printing nozzle and a triangular tip with a 15 nm radius of curvature. (b) The radial component of the field (magnitude and field lines shown) guide ejected droplets, which are charged, toward the tip. (c) Electron micrograph (top view) showing the deflection of printed CdSe/CdS quantum-dot lines when the printing nozzle is translated near the tip of a sharp template-stripped Au pyramid. (d) Electron micrograph (top view) of quantum-dot lines (arrows) printed along the apex of three neighboring template-stripped Au wedges. (e) Magnified electron micrograph of one of the quantum-dot lines in (d). (f) False-color fluorescence image of the line from (e) illuminated with UV light taken with a cooled sCMOS camera (Hamamatsu Flash 4.0, pixel size 6.5 μm). The quantum dots have a fluorescence peak at 629 nm.

further, as demonstrated in Figure 3. By diluting the ink, translating the piezo-stage quickly (200 μm per second), and using a relatively low ejection voltage (150 V), we obtained spots of only 30 nm (each containing 10–15 quantum dots, see Figure 3c). If the voltage was increased to 230 V (which decreases the ejected droplet size) sparse lines consisting of only a few or even single quantum dots were achieved (Figure 3d). At this limit, statistical fluctuations in the number of quantum dots in each printed droplet become relevant.

All of the above deposits are on flat substrates. As already mentioned, a greater challenge is to place quantum dots at specific positions on structured substrates. EHD NanoDrip printing can accomplish this task, in many cases even more readily than on flat substrates. In particular, on metallic structures, the nanocrystals can be preferentially guided toward positions where the local electromagnetic fields are the highest. This occurs due to the influence of the strong electrostatic fields at the nozzle. The ejected droplets, which have a high

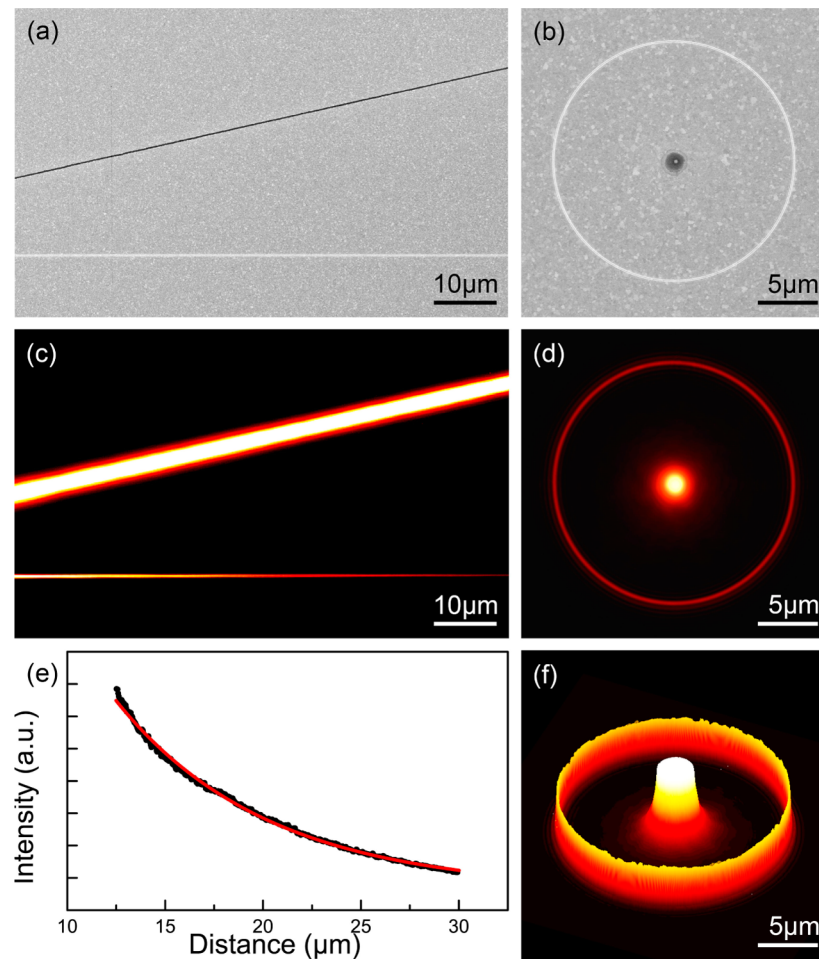


Figure 5. Hybrid quantum-dot-plasmonic circuits. (a) Electron micrograph (top view) of a line of CdSe/CdS core/shell quantum dots (dark tilted line) printed as a plasmon source on a flat template-stripped Au film. A Au bump line (bright horizontal line) is used as a scattering center. (b) Electron micrograph as in (a) but with a quantum-dot spot printed at the center of a circular Au bump line. (c) A false color optical micrograph taken with a cooled sCMOS camera and (d) a real color optical micrograph taken with a digital camera (Nikon D800) when the circuits in (a) and (b) were illuminated with UV light. The quantum dots emit photons into the far field (at 629 nm) and launch surface plasmon polaritons across the Au film, causing both fluorescence from the quantum-dot lines and scattered light from the bump lines. (e) The intensity of the scattered light from the bump line in (c) measured with a cooled sCMOS camera versus the distance between the bump and the quantum-dot line. The data (black points) are fit to an exponential decay (red line) for a surface plasmon propagation length of 7.8 μm . (f) Three-dimensional contour plot of the scattered light from the bump line in (d) measured with a cooled sCMOS camera. The scattered signal is uniform within 5%.

charge-to-mass ratio, will track electric field lines. Because electrostatic and electromagnetic fields have similar characteristics (particularly in the near field), the nozzle-to-substrate field lines will terminate where both have maxima. Thus, for sharp plasmonic structures such as pyramids or wedges, the ejected droplet will be guided to plasmonic “hot spots” that exist at tips or edges.^{32,34} This possibility can be seen in axis-symmetric electrostatic simulations (Figure 4a), which show the electric field lines between a nozzle and a conical tip. The radial component of the electric field (Figure 4b) will cause an “auto focusing” of the droplet during flight.³⁷ Indeed, this effect was confirmed in experiments (Figure 4c) that attempted to print a series of parallel quantum-dot lines across a Au template-stripped pyramid.⁴³ The lines were clearly deflected toward the sharp tip of the pyramid due to the electrostatic guiding. Because the electromagnetic mode density, and hence also the light-matter interactions, are expected to be highest at the tip, guiding the quantum dots toward this location is extremely useful.

In Figure 4d, we exploit this autofocusing to print quantum dots exactly along the apex of a metallic wedge. Three lines of quantum dots were placed on three successive wedges on a Au film. A higher-magnification image of one of the lines is shown in Figure 4e. The quantum dots are deposited with a resolution of \sim 100 nm and an even higher placement accuracy (limited to \sim 10 nm by the piezo-stage). The ability to position the active material at this scale is useful in many nanophotonic structures. For example, a strongly confined waveguide mode exists for SPPs along the apex of metallic wedges.^{32,44–46} If the quantum dots are placed in the near field of the apex, they can be illuminated with UV light (Figure 4f) to selectively excite this waveguide mode. Such far-field excitation of localized electromagnetic resonances can lead to new capabilities, as we now demonstrate with a few simple examples of quantum-dot-plasmonic circuits.

For circuits, one must be able to integrate active components (such as sources) with passive components (such as guides). In our case, we accomplished this with a two-step process. First, we structured the plasmonic substrate via template stripping.⁴³

For example, we placed grooves on the surface of a (001)-oriented Si wafer with focused-ion-beam (FIB) milling. A 250 nm thick Au layer was then evaporated and stripped off using an epoxy/glass substrate to reveal a smooth patterned Au film. In this process, the initial grooves in the Si template were transformed into bumps in the Au (the bright lines in Figure 5a,b). Second, we printed the active quantum-dot sources onto these patterned Au substrates (the dark lines in Figure 5a,b). By illuminating the quantum dots with UV light, SPPs should then be generated that propagate across the film. When they contact the bumps, photons should be scattered into the far field, which can be detected by a camera.

Using this approach, we created simple quantum-dot structures that generate both planar and spherical plasmonic waves. These could then be analyzed via their scattering signal to obtain information about the propagation characteristics and spatial distribution of the SPPs. In our first example, we printed a quantum-dot line at an angle to a linear Au bump (Figure 5a). By illuminating the quantum dots, this line can provide a linear, homogeneous photon source, as seen by the bright line in the fluorescence image in Figure 5c. In addition, SPPs should be generated that propagate from the quantum dots across the metal surface toward the Au bump. Indeed, the image in Figure 5c also shows light scattered from the bump, presumably due to this SPP propagation. To confirm this, we plotted the intensity of the scattered light from the bump versus its distance from the quantum-dot line (Figure 5e). The quality of the device allows us to measure this intensity with extremely high signal-to-noise. We observe an exponential decrease with a decay constant of $7.8 \mu\text{m}$. We also measured the propagation lengths for surface plasmon polaritons on similar Au films using the slit-groove technique,⁴³ and values of 7 to $8 \mu\text{m}$ were obtained.⁴⁷ Thus, we conclude that far-field excitation of printed quantum dots can easily produce near-field sources of SPPs.

In our second example, we printed a quantum-dot spot in the middle of a circular Au bump (Figure 5b). Upon UV illumination, these quantum dots should generate a spherical, plasmonic wave-pattern that propagates out from a point. Such waves should be uniform in intensity in any direction. As can be seen in the optical micrograph in Figure 5d, the scattered light from the circular bump is extremely uniform. This is also seen in Figure 5f, where the scattered intensity is plotted as a three-dimensional contour plot, and in Figure S4 in the Supporting Information, where it is shown as a polar plot. The observed uniformity not only confirms the generation of spherical waves but also the ability to place the quantum dots precisely at the center of the Au bump circle.

In conclusion, we have demonstrated a simple method for near-field light design for nanophotonics. We used electrohydrodynamic NanoDrip printing^{37,38} to place highly fluorescent quantum-dot patterns with arbitrary color, shape, and intensity with subdiffraction resolution and nanometer precision on planar and structured substrates. The deposits involve a countable number of quantum dots, which can be electrostatically guided toward electromagnetic hotspots on structured plasmonic substrates. Hybrid quantum-dot-plasmonic circuits can be easily created that generate, guide, and out-couple surface plasmon polaritons. In such circuits, the quantum dots act as local plasmonic sources when illuminated with ultraviolet light from the far field. Thus, a method for near-field light design is provided without the constraints of earlier techniques for integrating quantum dots into nanophotonic devices.

■ ASSOCIATED CONTENT

■ Supporting Information

Experimental methods and additional figures on EHD NanoDrip printing, the optical characterization, the synthesis of the quantum-dot inks, and the microfabrication of the plasmonic films. This material is available free of charge via the Internet at <http://pubs.acs.org>.

■ AUTHOR INFORMATION

Corresponding Author

*E-mail: dnorris@ethz.ch.

Notes

The authors declare the following competing financial interest(s): Two of the authors (Prof. Dimos Poulikakos and Dr. Patrick Galliker) are involved in a startup company that is attempting to commercialize the printing process used in our manuscript.

■ ACKNOWLEDGMENTS

We gratefully acknowledge assistance from V. Holmberg, K. McPeak, S. Meyer, and A. Sahu. The research leading to these results has received funding from the European Research Council under the European Union's Seventh Framework Programme (FP/2007-2013)/ERC Grant Agreement 339905 (QuaDoPS Advanced Grant) and from the Swiss National Science Foundation under Grant 146180.

■ REFERENCES

- (1) Klimov, V. I. *Nanocrystal Quantum Dots*, 2nd ed.; CRC Press: Boca Raton, 2010.
- (2) Norris, D. J.; Bawendi, M. G.; Brus, L. E. Optical properties of semiconductor nanocrystals (quantum dots). In *Molecular Electronics*; Jortner, J., Ratner, M., Eds.; Blackwell Science: Oxford, 1997; p 281.
- (3) Hines, M. A.; Guyot-Sionnest, P. *J. Phys. Chem. B* **1998**, *102*, 3655.
- (4) Banin, U.; Lee, C. J.; Guzelian, A. A.; Kadavanich, A. V.; Alivisatos, A. P.; Jaskolski, W.; Bryant, G. W.; Efros, A. L.; Rosen, M. J. *Chem. Phys.* **1998**, *109*, 2306.
- (5) Murray, C. B.; Sun, S.; Gaschler, W.; Doyle, H.; Betley, T. A.; Kagan, C. R. *IBM J. Res. Dev.* **2001**, *45*, 47.
- (6) Wehrenberg, B. L.; Wang, C. J.; Guyot-Sionnest, P. *J. Phys. Chem. B* **2002**, *106*, 10634.
- (7) Anikeeva, P. O.; Halpert, J. E.; Bawendi, M. G.; Bulović, V. *Nano Lett.* **2009**, *9*, 2532.
- (8) Shirasaki, Y.; Supran, G. J.; Bawendi, M. G.; Bulović, V. *Nat. Photonics* **2012**, *7*, 13.
- (9) Bruchez, M.; Moronne, M.; Gin, P.; Weiss, S.; Alivisatos, A. P. *Science* **1998**, *281*, 2013.
- (10) Michalet, X.; Pinaud, F. F.; Bentolila, L. A.; Tsay, J. M.; Doose, S.; Li, J. J.; Sundaresan, G.; Wu, A. M.; Gambhir, S. S.; Weiss, S. *Science* **2005**, *307*, 538.
- (11) Novotny, L.; Hecht, B. *Principles of Nano-Optics*; Cambridge University Press: Cambridge, U.K., 2012.
- (12) Genet, C.; Ebbesen, T. W. *Nature* **2007**, *445*, 39.
- (13) Lal, S.; Link, S.; Halas, N. J. *Nat. Photonics* **2007**, *1*, 641.
- (14) Gramotnev, D. K.; Bozhevolnyi, S. I. *Nat. Photonics* **2010**, *4*, 83.
- (15) Anker, J. N.; Hall, W. P.; Lyandres, O.; Shah, N. C.; Zhao, J.; Van Duyne, R. P. *Nat. Mater.* **2008**, *7*, 442.
- (16) Gordon, R.; Sinton, D.; Kavanagh, K. L.; Brolo, A. G. *Acc. Chem. Res.* **2008**, *41*, 1049.
- (17) Stewart, M. E.; Anderton, C. R.; Thompson, L. B.; Maria, J.; Gray, S. K.; Rogers, J. A.; Nuzzo, R. G. *Chem. Rev.* **2008**, *108*, 494.
- (18) Luk'yanchuk, B.; Zheludev, N. I.; Maier, S. A.; Halas, N. J.; Nordlander, P.; Giessen, H.; Chong, C. T. *Nat. Mater.* **2010**, *9*, 707.

- (19) Kalkbrenner, T.; Ramstein, M.; Mlynek, J.; Sandoghdar, V. *J. Microsc.* **2001**, *202*, 72.
- (20) Anger, P.; Bharadwaj, P.; Novotny, L. *Phys. Rev. Lett.* **2006**, *96*, 113002.
- (21) Novotny, L.; Stranick, S. J. *Annu. Rev. Phys. Chem.* **2006**, *57*, 303.
- (22) Bao, W.; Melli, M.; Caselli, N.; Riboli, F.; Wiersma, D. S.; Staffaroni, M.; Choo, H.; Ogletree, D. F.; Aloni, S.; Bokor, J.; Cabrini, S.; Intonti, F.; Salmeron, M. B.; Yablonovitch, E.; Schuck, P. J.; Weber-Bargioni, A. *Science* **2012**, *338*, 1317.
- (23) Raether, H. *Surface Plasmons*; Springer-Verlag: Berlin, 1988.
- (24) Barnes, W. L.; Dereux, A.; Ebbesen, T. W. *Nature* **2003**, *424*, 824.
- (25) Maier, S. A. *Plasmonics: Fundamentals and Applications*; Springer Science: New York, 2007.
- (26) Akimov, A. V.; Mukherjee, A.; Yu, C. L.; Chang, D. E.; Zibrov, A. S.; Hemmer, P. R.; Park, H.; Lukin, M. D. *Nature* **2007**, *450*, 402.
- (27) Kim, L.; Anikeeva, P. O.; Coe-Sullivan, S. A.; Steckel, J. S.; Bawendi, M. G.; Bulović, V. *Nano Lett.* **2008**, *8*, 4513.
- (28) Kim, T.-H.; Cho, K.-S.; Lee, E. K.; Lee, S. J.; Chae, J.; Kim, J. W.; Kim, D. H.; Kwon, J.-Y.; Amaralunga, G.; Lee, S. Y.; Choi, B. L.; Kuk, Y.; Kim, J. M.; Kim, K. *Nat. Photonics* **2011**, *5*, 176.
- (29) Tang, Z.; Ozturk, B.; Wang, Y.; Kotov, N. A. *J. Phys. Chem. B* **2004**, *108*, 6927.
- (30) Curto, A. G.; Volpe, G.; Taminiua, T. H.; Kreuzer, M. P.; Quidant, R.; van Hulst, N. F. *Science* **2010**, *329*, 930.
- (31) Bermúdez Ureña, E.; Kreuzer, M. P.; Itzhakov, S.; Rigneault, H.; Quidant, R.; Oron, D.; Wenger, J. *Adv. Mater.* **2012**, *24*, OP314.
- (32) Moreno, E.; Rodrigo, S.; Bozhevolnyi, S.; Martín-Moreno, L.; García-Vidal, F. *Phys. Rev. Lett.* **2008**, *100*, 023901.
- (33) Schuller, J. A.; Barnard, E. S.; Cai, W. S.; Jun, Y. C.; White, J. S.; Brongersma, M. L. *Nat. Mater.* **2010**, *9*, 193.
- (34) Lindquist, N. C.; Nagpal, P.; Lesuffleur, A.; Norris, D. J.; Oh, S. H. *Nano Lett.* **2010**, *10*, 1369.
- (35) Juan, M. L.; Righini, M.; Quidant, R. *Nat. Photonics* **2011**, *5*, 349.
- (36) Geiselmann, M.; Marty, R.; Renger, J.; de Abajo, F. J. G.; Quidant, R. *Nano Lett.* **2014**, *14*, 1520.
- (37) Galliker, P.; Schneider, J.; Eghlidi, H.; Kress, S.; Sandoghdar, V.; Poulikakos, D. *Nat. Commun.* **2012**, *3*, 890.
- (38) Galliker, P.; Schneider, J.; Poulikakos, D. *Appl. Phys. Lett.* **2014**, *104*, 073105.
- (39) Reiss, P.; Bleuse, J.; Pron, A. *Nano Lett.* **2002**, *2*, 781.
- (40) Dethlefsen, J. R.; Dossing, A. *Nano Lett.* **2011**, *11*, 1964.
- (41) Chen, O.; Zhao, J.; Chauhan, V. P.; Cui, J.; Wong, C.; Harris, D. K.; Wei, H.; Han, H. S.; Fukumura, D.; Jain, R. K.; Bawendi, M. G. *Nat. Mater.* **2013**, *12*, 445.
- (42) Hegner, M.; Wagner, P.; Semenza, G. *Surf. Sci.* **1993**, *291*, 39.
- (43) Nagpal, P.; Lindquist, N. C.; Oh, S. H.; Norris, D. J. *Science* **2009**, *325*, 594.
- (44) Pile, D. F. P.; Ogawa, T.; Gramotnev, D. K.; Okamoto, T.; Haraguchi, M.; Fukui, M.; Matsuo, S. *Appl. Phys. Lett.* **2005**, *87*, 061106.
- (45) Boltasseva, A.; Volkov, V. S.; Nielsen, R. B.; Moreno, E.; Rodrigo, S. G.; Bozhevolnyi, S. I. *Opt. Express* **2008**, *16*, 5252.
- (46) Martin-Cano, D.; Martin-Moreno, L.; Garcia-Vidal, F. J.; Moreno, E. *Nano Lett.* **2010**, *10*, 3129.
- (47) The theoretical values (assuming only Ohmic losses) expected for the propagation lengths at 610, 630, and 650 nm are 8.5, 12.2, and 17.2 μm , respectively, based on the measured dielectric functions for our Au films.